

# Studies of ETB Evolution and Stability on COMPASS-D Tokamak

FIELD A.R.\* , CAROLAN P.G., CONWAY N.J., FIELDING S.J.,  
HELANDER P., JONES P.B.<sup>1</sup>, MEYER H.F. and POGUTSE O.  
EURATOM / UKAEA Fusion Association, Culham Science Centre,  
Abingdon, Oxon, OX14 3DB, UK

<sup>1</sup> Department of Physics, Imperial College of Science, Technology & Medicine,  
Prince Consort Road, London, SW7 2BZ, UK

(Received: 5 December 2000 / Accepted: 16 August 2001)

## Abstract

Detailed, coincident measurements of several plasma edge parameters on COMPASS-D tokamak have been made using a novel combined spectroscopic diagnostic comprising a thermal helium beam and Doppler spectrometer. These measurements have enabled progress to be made both in assessing theories of the L/H-transition and ETB stability and in investigating the evolution of the radial electric field and the local neutral density in the region of the ETB. This has enabled controversial issues such as the role of neutral particles and the causality of events to be addressed.

## Keywords:

tokamak, ETB, L/H-transition, peeling, Alfvén-drift, neo-classical, radial E-field, shear, neutral

## 1. Introduction

There are many theories for the L- to H-mode transition [1] but none is universal. Experimental tests of such theories require detailed measurements able to follow the rapid ( $\leq$  ms) changes in edge parameters which occur at L- to H-transitions over the small spatial scale ( $\leq$  cm) of the ETB. On COMPASS-D tokamak a novel combination of spectroscopic diagnostics [2] is able to provide coincident measurements of several edge parameters. Such measurements are used to assess theories of ETB formation [2] by evaluating specific normalised parameters, which define the stability regime of a particular instability, turbulence mechanism or other H-mode trigger, and comparing observed thresholds with predicted transition criteria. The combined spectroscopic data are also sufficient to determine the evolution of the radial electric field and the neutral density. Thereby, controversial issues such as the role of neutral

particles and the causality of events are investigated by studying controlled L/H- and H/L-transitions in discharges exhibiting a sequence of such transitions.

## 2. Experimental

A combination [3] of a thermal helium beam diagnostic (HELIOS) [4] and a Doppler spectrometer (CELESTE) [5] views the plasma boundary at the outboard mid-plane through common collection optics.  $T_e$  and  $n_e$  profiles are obtained from He I line intensity ratios measured by the HELIOS spectrometer at 10 radial locations ( $\Delta R = 5$  mm) using atomic data from ADAS [6]. Profiles of  $D\alpha$  intensity are also measured using the same spectrometer. The time resolution is typically 5 ms ( $\geq 2$  ms). The high-resolution CELESTE spectrometer measures profiles of impurity line emission on 19 lines of sight ( $2$  mm  $\leq \Delta R \leq 5$  mm) with a temporal

\*Corresponding author's e-mail: Anthony.Field@ukaea.org.uk

resolution  $\Delta t$  of 2.5ms. The amplitude, width and wavelength shift of the line give the relative intensity  $I_z$  and impurity temperature  $T_z$ , and poloidal velocity  $v_{\theta z}$  respectively. The He II (468.6nm) resonance line is used here as the emission is essentially localised to the helium beam, the ionisation length for these ions ( $\lambda_{\text{ion}} \approx 3\text{m}$ ) being shorter than the toroidal circumference of COMPASS-D (4.6m).

### 3. ETB Stability

In order to investigate the stability of the ETB specific normalised parameters required for comparison with theory are evaluated from the edge measurements. For example, as shown in Fig. 1 (a), plots of normalised edge electron pressure gradient  $\alpha_e = -Rq^2\beta'$  against edge collisionality  $\nu_e^* = 8.36 \times 10^{-5} \ln \lambda R q n_e (10^{19} \text{m}^{-3}) / e^{3/2} T_e^2$  (keV) show that H-mode is confined to a region where

both  $\alpha_e$  and  $\nu_e^*$  exceed critical values. L-H transition points lie on or close to the boundaries (significantly, as do those points which encompass ELMs during the measurement interval), consistent with stabilisation of the peeling mode as a necessary condition for H-mode. The peeling mode is driven by edge current and stabilised by edge pressure gradient [7], and at sufficiently low density, and correspondingly low collisionality, the bootstrap current drive always exceeds the stabilising effect of the pressure gradient. Above a certain collisionality  $\nu_e^* > 1$  which sets the low density limit to the H-mode, the bootstrap current is reduced and the peeling mode can be stabilised provided the edge pressure gradient is sufficiently high.

Limiting boundaries at the L-H transition also appear in edge parameter plots characterising theoretical models of turbulence suppression mechanisms. Three-dimensional, non-linear simulations of drift-ballooning modes in a torus [8] indicate that the effect of electromagnetic fluctuations is to significantly enhance transport when  $\alpha_e$  exceeds a critical value well below the ballooning limit, unless diamagnetic effects are strong. Diamagnetic effects are characterised by the parameter  $\alpha_{\text{dia}} = (2\pi q)^{-1} (m_i/2m_e)^{1/4} (v_{\text{th},e}/(v_{e,i}\sqrt{RL_n}))^{1/2}$  where  $v_{\text{th},e}$  is the electron thermal velocity and  $v_{e,i}$  the electron-ion collision frequency. For sufficiently high  $\alpha_e > 0.5$  strong sheared poloidal flow develops when  $\alpha_{\text{dia}} > 0.75$  which suppresses turbulent transport. As shown in Fig. 1(b), there is a critical  $\alpha_e$  for the occurrence of H-mode but there is no evidence for a correlation with  $\alpha_{\text{dia}}$ , which exceeds 0.75 under all conditions indicating that this mechanism is not controlling the L-H transition.

Recent theoretical studies of Alfvén-drift wave turbulence suppression [9] indicate that as the edge electron diamagnetic-drift velocity increases, interaction between electron drift waves and Alfvén waves can suppress the long wavelength drift-waves thought to be responsible for edge transport. The criterion for turbulence suppression is  $\beta_n > 1 + \nu_n^{2/3}$ , where  $\beta_n \propto \alpha_e / r q'$  and  $\nu_n$  is the normalised electron collision frequency. A plot of  $\beta_n/(1 + \nu_n^{2/3})$  against  $\nu_n$  for COMPASS-D data in Fig. 1 (d) indeed shows that there is a critical value of this parameter of  $\approx 2$ , at the L-H transition. Furthermore, this plot exhibits one significant difference from the three others, in that data from dithering sections of the L-H transition are clearly separated from L-mode data. As soon as 'dithers' are observed in the  $D\alpha$  signal, evidence of a sporadic improvement in particle transport prior to formation of the stable transport barrier,  $\beta_n$  is seen to increase. This 'precursor'

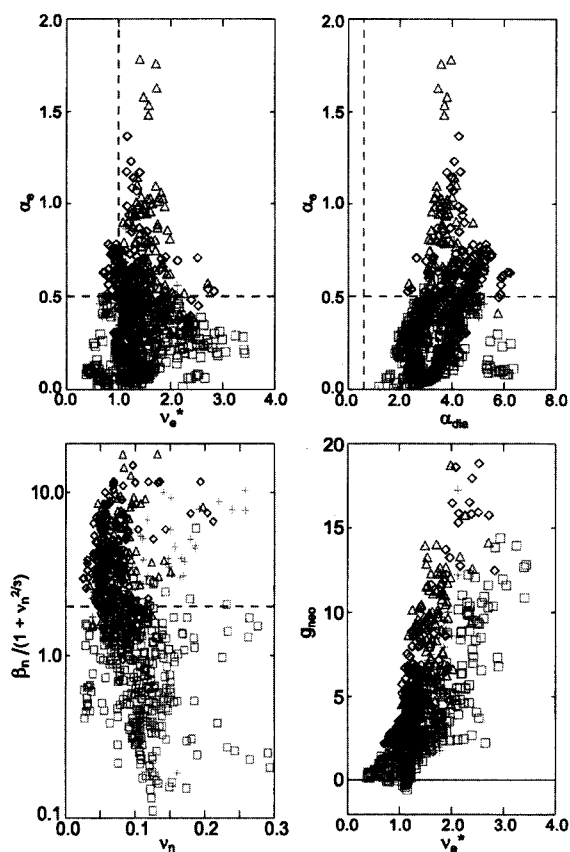


Fig. 1 Stability plot for various theories of edge instabilities and transport: (a) 'peeling' mode; (b) drift-ballooning turbulence; (c) drift-Alfvén turbulence suppression; (d) neo-classical transport in impure plasma. Data points are during L- ( $\square$ ), H- ( $\Delta$ ), ELMy- ( $\diamond$ ) or dithering (+) H-mode and are evaluated at the 90% flux surface.

behaviour indicates that suppression of this turbulence occurs particularly early in the transition evolution and may act as a controlling trigger. This mechanism is an attractive candidate since it is also consistent with data from a wide range of tokamaks and can be formulated [10] to predict the difference in density and magnetic field scalings for the L-H power threshold which are observed between COMPASS-D and other devices. This results from different scalings of  $\chi_{||}$  which occur in different collisionality regimes at the plasma edge [11]. In particular, the predicted scaling in COMPASS-D  $P_{th} \propto B^3/n^{1.5}$  agrees closely with that observed  $P_{th} \propto B^{3.6}/n^{1.5}$  [2].

Another possible effect giving rise to a confinement transition is a bifurcation in the underlying neo-classical transport, with a reduction in radial particle transport occurring with sufficiently steep edge gradients. An extension of the neo-classical theory of an impure plasma [12] into such regimes predicts that as  $\delta$  ( $\approx \rho_{i\theta}/L_{\perp}$ , where  $L_{\perp}$  is a radial scale length,) increases a poloidal asymmetry should develop in the impurity density which will in turn reduce the parallel impurity friction and thus reduce the radial particle flux. Characterising the gradients by the parameter:  $g_{neo} = Z^2 \hat{v}_{ii} \rho_{\theta i} (1/L_{ni} - 1/2L_{Ti})$ , where  $Z$  is the dominant impurity charge, it can be shown that a reduction in the radial particle flux should occur with increasing gradients provided  $g_{neo}$  exceeds a critical value  $\approx 2$ . As shown in Fig. 1 (c), which plots  $g_{neo}$  against  $v_e^*$  from COMPASS-D discharges, assuming equal ion and electron temperatures and  $Z = 5$  (representative low  $Z$  impurity), there is a critical  $g_{neo}$  for formation of the H-mode  $\approx 2-5$ .

#### 4. ETB Evolution

In order to study the formation, evolution and decay of the ETB in detail discharges are set up where L/H- and H/L-transitions are triggered by controlling the gas fuelling. Fig. 2 shows time traces for shot #28448 of the poloidal  $He^+$  drift velocity on surfaces of constant poloidal flux, the  $D\alpha$  intensity and the gas puff reference voltage. Prior to the L/H-transition the plasma is in L-mode close to the transition threshold. Termination of the gas fuelling at 155ms causes a transition to the ELM-free H-mode indicated by a sudden drop in the  $D\alpha$  intensity. A stepped gas puff is applied at 170ms the initial phase triggering an H/L-transition which is sustained by the smaller latter phase. Once the gas puff is terminated the plasma again enters ELM-free H-mode.

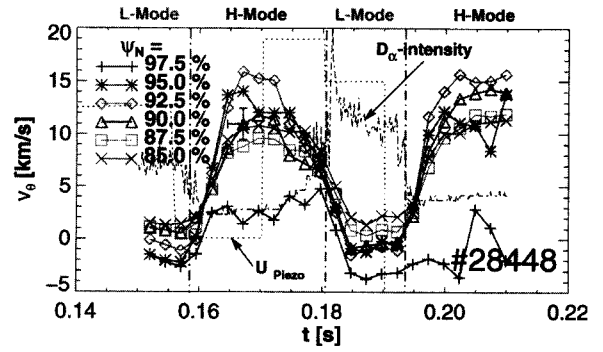


Fig. 2 The time evolution of the poloidal velocity of the  $He^+$  ions along surfaces of constant poloidal flux for shot #28448. The  $D\alpha$  intensity and the gas puff drive are also shown.

In the initial L-mode phase there is little velocity shear evident, the strong shear evolving only *after* the L-H transition and the velocity showing a maximum in H-mode around the 93% flux surface. Following the gas puff at 170ms the shear is reduced, leading to an H-L transition when the shear within the ETB is virtually removed. In the subsequent L-mode phase the rotation is rapidly suppressed. When the gas puff is again turned off the second L-H transition is initiated and the poloidal velocity and its shear increase as before.

As the  $He^+$  impurity ion velocity can differ substantially from that of the main ions it is useful to determine the radial electric field which all ion species experience. (Quantities are represented in terms of the flux coordinates ( $\psi, \theta, \phi$ ) where  $\psi$  is the poloidal flux,  $\theta$  the poloidal angle and  $\phi$  the toroidal angle.) The radial electric field  $E_{\psi}$  is computed from the approximate radial momentum balance of the impurity species:

$$E_{\psi} = \frac{\nabla p_z \cdot \nabla \psi}{Z_z e n_z |\nabla \psi|} - v_{z\theta} B_{\phi} \quad (2)$$

The first term on the right hand side is the diamagnetic contribution, depending on the impurity temperature and the gradient scale lengths of  $T_z$  and  $n_z$ . The latter has to be derived from the measured intensity by using ADAS data [6] as well as  $T_e$  and  $n_e$ . Additional terms due to toroidal rotation, inertia, perpendicular viscosity, neutral friction and coulomb friction are neglected as these are small ( $< 10\%$ ) compared with the diamagnetic term.

Inside the last closed flux surface  $E_{\psi}$  is negative with higher values in H-mode compared to L-mode and a maximum change of  $\Delta E_{\psi}$  of  $-12\text{ kV/m}$ . As shown in Fig. 3 the region of maximum shear  $\partial E_{\psi} / \partial r \approx 2 \times 10^3 \text{ kV/m}^2$  is located close to the 96% flux surface. In the L-

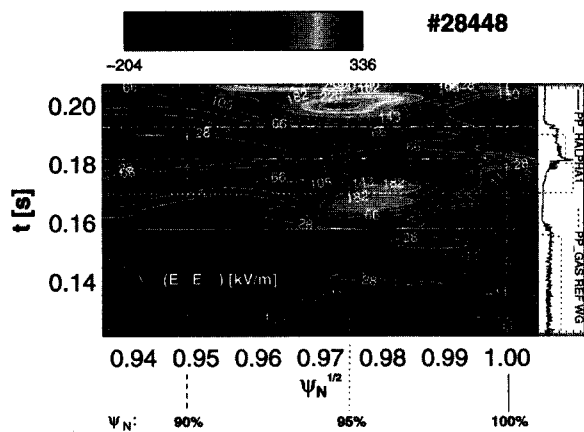


Fig. 3 The evolution of the profile of the shear in  $E_y$  relative to the average shear over the L-mode phase (140–155ms) for shot #28448 with  $\psi_N \sim r/a$  as abscissa. The locations of the 90, 95 and 100% flux surfaces are marked as well as the transition times. The  $D\alpha$  intensity and the gas puff waveforms are also shown.

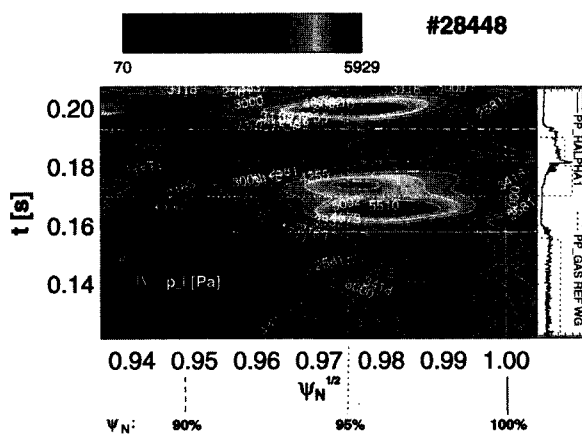


Fig. 4 A similar plot to Fig. 3 of the electron pressure gradient  $\partial p_e / \partial \psi_N$  for shot #28448.

mode phase  $E_y$  already exhibits shear although shear in  $v_{z\theta}$  is negligible. After the L/H-transition the shear in  $E_y$  increases. After the onset of the gas puff the shear starts to decrease *before* the H/L-transition which occurs when the shear is almost removed. The electron pressure gradient shown in Fig. 4 steepens after the L/H-transition and exhibits a maximum, corresponding to the location of the ETB, which is coincident with the maximum gradient of  $E_y$ . As shown in Fig. 5, during the H-mode phases, changes in  $(\partial E_y / \partial \psi_N)^{\max}$  relative to L-mode increase with  $|\partial p_e / \partial \psi_N|^{\max}$  indicating that increased shear of  $E_y$  is associated with a reduction of

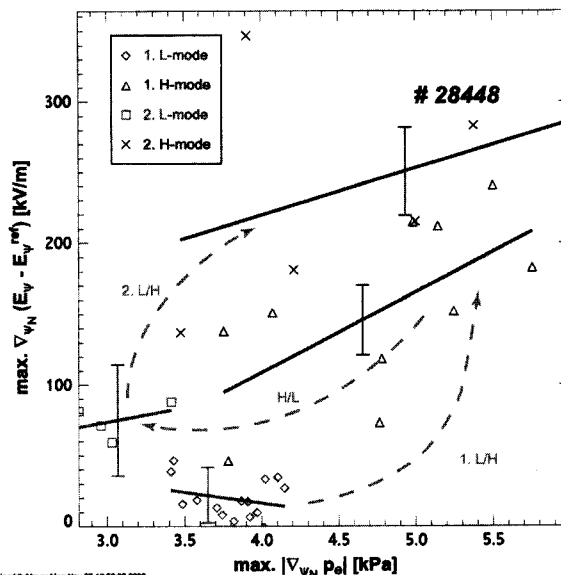


Fig. 5 Dependence of the change in the maximum  $\partial E_y / \partial \psi_N$  relative to L-mode phase on the maximum of  $\partial p_e / \partial \psi_N$  for the two H- and L-phases of shot #28448.

electron transport within the ETB. Measurements of the background-ion pressure gradient are not available.

The electron density inside the separatrix is higher in the H-mode than in the L-mode but reduced outside in the SOL. The converse is true for the neutral density, which is determined from a spatial inversion of the absolute  $D\alpha$  intensity profile [13] using the collisional radiative model of Fujimoto *et al.* [14]. During the L-mode the neutrals extend further into the plasma than in the H-mode. Changes in  $n_D$  follow the transitions whereas changes in  $n_e$  correlate with those of  $E_y$ .

## 5. Conclusions

High resolution edge measurements in the region of the ETB on COMPASS-D enable the behaviour of derived normalised parameters to be compared with a variety of transition theories/models. Four of these are shown to have stability regimes whose limiting boundaries are not inconsistent with the L/H-transition boundaries. This suggests that all these turbulence mechanisms may have to be stabilised for ETB formation but does not identify the controlling mechanism. A theory based upon Alfvén-drift-wave turbulence suppression is attractive because the data exhibit precursor behaviour in its stability regime and it can be formulated to give density and magnetic field dependencies in agreement with the very different global power scalings observed

on COMPASS-D and with the ITER scalings.

Detailed measurements of the evolution of the poloidal velocity and associated radial electric field throughout periods of L- and H-mode have shown that significant shear develops in these quantities only after the L/H-transition. This is in contrast to observations on other machines [15] and may be linked to the different trigger mechanisms which control the transition in different regimes. When gas puffing is used to trigger a reversed H/L-transition, reduction in shear occurs before the transition, which takes place when the shear is reduced to its L-mode value. The region of maximum shear correlates with the maximum electron pressure gradient. The observation that changes in the local neutral density occur only after the H/L- and L/H-transitions does not support a local influence of  $n_D$  on shear.

### References

- [1] J.W. Connor and H. Wilson, Plasma Phys. Contr. Fusion **42**, (2000).
- [2] S.J. Fielding *et al.*, 25th EPS Conf. on Control. Fusion Plasma Phys. (Prague, Czech Rep. 1998) B092.
- [3] P.G. Carolan, N.J. Conway, A.R. Field and H.F. Meyer, Synergy of multi-viewing diagnostics on COMPASS-D, Rev. Sci. Instrum. **72** (1) Part 11, 881 (2001).
- [4] A.R. Field, P.G. Carolan, N.J. Conway and M.G. O'Mullane, Rev. Sci. Instrum. **70** (11), 355 (1999).
- [5] P.G. Carolan, N.J. Conway, C.A. Bunting, P. Leahy *et al.*, Rev. Sci. Instrum. **68** (1), 1015 (1997).
- [6] H.P. Summers, Atomic data and analysis structure, JET Report JET-IR(94) 06 (1994).
- [7] J.W. Connor, R.J. Hastie, H.R. Wilson and R.L. Miller, Phys. Plasmas **5**, 2687 (1998).
- [8] B.N. Rogers and J.F. Drake, Phys. Rev. Lett. **79**, 229 (1997).
- [9] O. Pogutse, Yu. Ighitkahnov *et al.*, 24th EPS Conf. on Control. Fusion Plasma Phys. (Berchtesgaden, Germany 1997) 21 AIII p.1545.
- [10] Yu Ighitkhanov *et al.*, 27th EPS Conf. on Control. Fusion Plasma Phys. (Budapest, Hungary 2000) P1 039.
- [11] J.W. Connor *et al.*, Nucl. Fusion **39**, 169 (1999).
- [12] P. Helander, Phys. Plasmas **5**, 3999 (1998).
- [13] H. Meyer, P.G. Carolan, N.J. Conway, A.R. Field, S.J. Fielding, P. Helander and P.B. Jones, 'Profile evolution of edge parameters during L/H- and H/L-mode transitions in COMPASS-D', 3<sup>rd</sup> Europhysics Workshop on 'Role of Electric Fields in Plasma Confinement and Exhaust', 18<sup>th</sup> – 19<sup>th</sup> June '00, Budapest, Hungary, to be published in Czechoslovak Journal of Physics.
- [14] K. Sawada, K. Eriguchi and T. Fujimoto, J. Appl. Phys. **73** (12), 8122 (1993).
- [15] K.H. Burrell, Phys. Plasmas **6** (12), 4418 (1999). *This work is funded jointly by the UK Department of Trade and Industry and EURATOM.*